DOI: 10.1021/ma102532k

Macromolecules
ARTICLE

Iodine Transfer Terpolymerization of Vinylidene Fluoride, α-Trifluoromethacrylic Acid and Hexafluoropropylene for Exceptional Thermostable Fluoropolymers/Silica Nanocomposites

Hideo Sawada,[†] Tsukasa Tashima,[†] Yusuke Nishiyama,[‡] Mieko Kikuchi,[†] Yuki Goto,[†] George Kostov,[§,∥] and Bruno Ameduri*[,§]

[†]*Department of Frontier Materials Chemistry, Graduate School of Science and Technology, Hirosaki University, Bunkyo-cho, Hirosaki 036-8561, Japan,* [‡]*JEOL, Ltd., Akishima, Tokyo 195-8558, Japan,* [§]*Ingénierie et Architectures Macromoléculaires, Institut Charles Gerhardt, Ecole Nationale Supérieure de Chimie de Montpellier (UMR 5253-CNRS), 8, rue de l'Ecole Normale, 34296 Montpellier Cedex 1, France, and* [∥]*Department of Organic Chemical Technology, Burgas Assen Zlatarov University, 1, Boulevard Prof. Yakimov, 8010 Burgas, Bulgaria*

Received November 6, 2010; Revised Manuscript Received January 10, 2011

ABSTRACT: The synthesis of poly(VDF-*ter*-TFMA-*ter*-HFP) terpolymers (where VDF, TFMA, and HFP stand for vinylidene fluoride, α-trifluoromethacrylic acid, and hexafluoropropylene, respectively) and their blends with silica filler for preparing original fluorocomposites are presented. First, the radical terpolymerization of VDF, TFMA, and HFP by iodine transfer polymerization without any surfactant was investigated in the presence of 1,6-diiodoperfluorohexane as the chain transfer agent. TFMA monomer was well incorporated, and the terpolymers were obtained in good yields (> 65%). The microstructures of the produced terpolymers were characterized by ^{1}H and ^{19}F NMR spectroscopy to assess the amounts of each comonomer, the molecular weights, and the nature of the end groups of the copolymers. Molar percentages of VDF, TFMA, and HFP were in the 45−80, 12−53, and 1−8 ranges, respectively, whereas the molecular weights of the resulting terpolymers were ca. 5400−12 600 g·mol^{-1}. End groups were VDF-I only with a high amount of CH_2CF_2−I. Then, these poly(VDF-*ter*-TFMA-*ter*-HFP) terpolymers were involved in the preparation of the fluorinated polymers/silica nanocomposites by sol−gel reactions in the presence of tetraethoxysilane and silica nanoparticles under alkaline and acidic conditions, respectively. Interestingly, poly(VDF-*ter*-TFMA-*ter*-HFP) terpolymer/silica nanocomposites, which were prepared under alkaline conditions, showed exceptional thermal properties because they were found to exhibit almost no weight loss up to 800 °C.

Introduction

Fluoropolymers exhibit unique and remarkable properties,[1−4] such as thermal stability, chemical inertness (to acids, bases, organic solvents), low refractive indices, dielectric constants, and dissipation factors, are hydrophobic, display excellent weathering capabilities, and show interesting surface properties. Hence, these high-value-added materials can find applications in many fields of high technology: aeronautics,[5] microelectronics,[6] optics,[7,8] textile finishing,[9,10] the nuclear industry,[11] paints and coatings,[12] photovoltaic devices,[13] and lithography.[14] These specialty polymers are usually produced by radical (co)polymerization of fluorinated monomers. Among these polymers, poly(vinylidene fluoride) (PVDF) plays an interesting role because its properties (such as the chemical inertness, the resistance to acids and to chemical agents, piezo-, pyroelectrical, and gas-barrier properties, and low toxicity) can be tuned and enhanced by the presence of specific functional groups born by the backbone,[15−17] that is, adhesion, solubility, cross-linkability, ion exchange, and so on. The strategy to insert functional groups in PVDF currently deals with the radical copolymerization of fluoroalkenes with a functional fluorinated or nonhalogenated monomers.

In fact, vinylidene fluoride (VDF) has been copolymerized with various fluorinated monomers,[4,16,17] and the resulting copolymers bear functionality such as hydroxy,[17] carboxylic acid,[18−20] acetoxy,[17] thioacetoxy,[17] sulfonyl fluoride,[17] nitrile,[17] trialkoxysilane,[21,22] bromine,[23] or a pentafluorosulfonyl[22] group.

An interesting way to insert a carboxylic acid function (which opens up to various further chemical modifications) arises from the copolymerization of VDF with comonomers containing such acid group. Actually, acrylic acid (AA) or methacrylic acid (MAA)[25] are too reactive (their propagation rates, k_p, are very high compared with that of VDF[26]) to lead to poly(VDF-*co*-(M)AA) copolymers containing a too-low content of VDF.[19] In contrast, α-trifluoromethacrylic acid (TFMA) does not homopolymerize under radical conditions[27,28] but has already evidenced a satisfactory reactivity with VDF.[18] In addition, its conventional free-radical terpolymerization with VDF and hexafluoropropylene (HFP)[18] was successfully carried out in organic solvent. Iodine transfer polymerization (ITP)[29] has been chosen because this is a suitable technique that is able to control the polymerization of fluorinated olefins.[30] Nanocomposites made of polymers have shown exceptional properties, but few fluoropolymer/nanofillers blends composites have been reported.[31] There is a real challenge to disperse nanofillers in fluorinated polymers, although examples on PVDF are scarce. Among them, PVDF/nanofiller or PVDF/clay nanocomposites have been investigated, and four examples are given hereafter. First, Lui et al.[32] studied the effect of montmorillonite clay containing various quaternary alkylammonium salts for the preparation of gel PVDF

*Corresponding author. Tel: +33-467-144-368. Fax: +33-467-147-220. E-mail:bruno.ameduri@enscm.fr.

 Published on Web 02/03/2011

nano-composite electrolytes for lithium ion batteries. The resulting materials showed better film formation, solvent-maintaining capability, and dimensional and electrochemical stabilities and enhanced ionic conductivity (reaching a value up to 10^3 $mS \cdot cm^{-1}$) than electrolyte films without any added organophilic clays. The same year, Priya and Jog[33] obtained PVDF/clay nanocomposites by melt intercalation with organophilic bentonite clay (Cloisite 6A-treated with dimethyl dehydrogenated allowed quaternary ammonium chloride) and noted three major features: (i) PVDF in the nanocomposites crystallized in the β form[33] (which was stable after thermal annealing[34]); (ii) an enhanced rate of crystallization with the addition of clay; and (iii) significant improvement in the storage modulus over the temperature range of −100 to 150 °C. Then, Dillon et al.[35] investigated the PVDF/nanoclay composites prepared by both solution casting and coprecipitation methods and using three nanoclay morphologies (exfoliated, partially intercalated, and phase-separated morphology). From solution cast samples, phase separation and intercalation occurred, depending on the organic modifiers, whereas complete exfoliation of the nanoclays was noted in the coprecipated nanocomposites. Chung's group[36] prepared nanocomposites on the basis of PVDF as an original "polymeric surfactant", which showed interfacial activity in the exfoliated fluoropolymer/clay nanocomposites.

Wu et al.[37] obtained matrices for high-conducting, low-leakage porous polymer electrolytes poly(VDF-*co*-HFP) copolymers/metaloides (TiO_2, MgO, ZnO, $BaTiO_3$) that led to original conducting porous polymer electrolytes with improved conductivity than that of pure poly(VDF-*co*-HFP) copolymers. In addition, PVDF composite membranes filled with different weight fractions of SiO_2 nanoparticles have been prepared by a blending method for organic−inorganic hybrid fuel cell membranes[38] that exhibit high thermal stability, improved selectivity, and moderate membrane conductivity and may be suitable for use in the electrodriven separation processes. A more recent strategy also led to fuel cell membranes from sol−gel process[39] involving poly(VDF-*ter*-VTEOS-*ter*-PFSVE) terpolymers (where VTEOS and PFSVE stand for vinyl triethoxysilane and perfluoro-(4-methyl-3,6-dioxaoct-7-ene) sulfonyl fluoride, respectively).

Many other groups also investigated the preparation of original composites made of PVDF and nanofillers[40−44] or in blends with poly(styrene)-*b*-poly(vinylpyridine)-*b*-poly(ethylene oxide) triblock tercopolymers.[45]

Recently, Sawada's group[46] has been able to encapsulate (or to blend) diamonds[47] or silica[48] with R_F-$(AA)_n R_F$ triblock cooligomers. No similar work involving copolymers based on VDF has already been achieved. However, few investigations on composites based on copolymer containing VDF and silica have been reported, and it was worth revisiting it. Hence, the objectives of this Article concern the preparation of stable fluoropolymer nanocomposites from mixing nanosilica with poly(VDF-*ter*-TFMA-*ter*-HFP) terpolymers.

Experimental Part

Materials. VDF (or 1,1-difluoroethylene, b.p. = −82 °C), HFP (b.p. = −28 °C), and TFMA were kindly offered by Solvay S.A. (Tavaux, France and Brussels, Belgium) and Tosoh F-Tech Company (Shunan, Japan), respectively. 1,6-Diiodoperfluorohexane was purchased at Ugarit (France). It was worked up with sodium thiosulfate and then distilled prior to use. $Na_2S_2O_8$ (purity 99%) was purchased from Aldrich. Acetonitrile, dimethylformamide (DMF), tetrahydrofuran (THF), methanol, methylethylketone, and dimethylacetamide (DMAc) of analytical grade were purchased from Aldrich Chimie, 38299 Saint Quentin-Fallavier, France. Silica-nanoparticle methanol solution [30 wt % average particle size: 11 nm (Methanol Silica-sol)] and tetraethoxysilane (TEOS) were supplied by Nissan Chemical Industrials, Tokyo, Japan and Tokyo Chemical Industrial (Tokyo, Japan), respectively. They were used as supplied.

Scheme 1. Iodine Transfer Terpolymerization of Vinylidene Fluoride, α-Trifluoromethacrylic Acid and Hexafluoropropylene Performed in the Presence of 1,6-Diiodoperfluorohexane

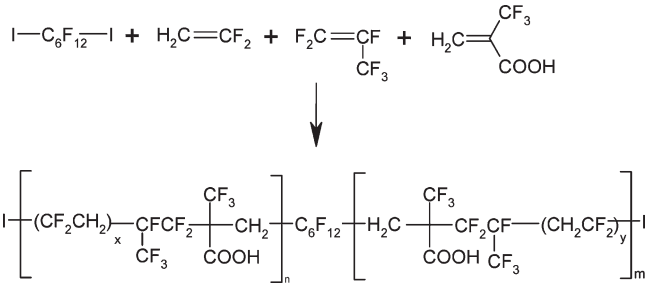

Analyses. The compositions and the structures of the diiodofluorotelechelic oligomers obtained by ITP were determined by ^{19}F and ^1H NMR spectroscopies. The NMR spectra were recorded on Bruker AC 250 or 400 (250 or 400 MHz) instruments using deuterated acetone, dimethylsulfoxide (DMSO) or DMF as the solvents and tetramethylsilane (TMS) (or $CFCl_3$) as the reference for ^1H (or ^{19}F) nuclei. Coupling constants and chemical shifts are given in hertz and ppm, respectively. The experimental conditions for ^1H (or ^{19}F) NMR spectra were the following: flip angle 90° (or 30°), acquisition time 4.5 s (or 0.7 s), pulse delay 2 s (or 5 s), number of scans 16 (or 64), and a pulse width of 5 s for ^{19}F NMR.

Size exclusion chromatography (SEC) analyses were performed with a Spectra-Physics apparatus equipped with two PLgel 5 μm Mixed-C columns from Polymer Laboratories and a Spectra Physics SP8430 refractive index (RI) detector. (The signals assigned to poly(VDF-*ter*-TFMA-*ter*-HFP)-I terpolymers gave negative values.) DMF containing 1.5 wt % LiCl was chosen as the eluent at T = 40 °C, with a flow rate of 0.8 mL min^{-1}. Monodispersed standards were poly(styrene)s purchased from Polymer Laboratories.

^{19}F magic-angle spinning (MAS) NMR spectra were recorded at room temperature using JEOL JNM-ECA500 with 3.2 mm ^{19}F MAS probe. Fourier-transform infrared (FTIR) spectra were measured using a Shimadzu FTIR-8400 FT-IR spectrophotometer (Kyoto, Japan). We recorded thermal analyses by increasing the temperature from room temperature to around 800 °C (at a heating rate of 10 °C/min) under atmospheric conditions by using a Bruker AXS TG-DTA2000SA differential thermobalance (Kanagawa, Japan). Dynamic light scattering (DLS) measurements were performed by means of an Otsuka Electronics DLS-7000 HL (Tokyo, Japan) apparatus. The zeta potential was assessed by the use of a Microtec Nition ZEECOM/ZC-2000 (Chiba, Japan) apparatus.

Field-emission scanning electron microscopy (FE-SEM) images were measured by using a JEOL JSM-5300 (Tokyo, Japan) apparatus.

Reaction in Autoclave. Iodine transfer terpolymerizations of VDF, TFMA, and HFP were carried out in deionized water in the presence of 1,6-diiodoperfluorohexane as the CTAs and initiated by $Na_2S_2O_8$ at 80 °C. A 160 mL Hastelloy (HC-276) autoclave, equipped with inlet and outlet valves, a manometer, and a rupture disk, was degassed and pressurized with 30 bar of nitrogen to check eventual leaks. Then, a 7 mmHg vacuum was operated for 30 min. Under vacuum, 0.904 g (0.0038 mol) of $Na_2S_2O_8$, 4.12 g (0.0075 mol) of 1,6-diiodoperfluorohexane, 10.22 g (0.073 mol) of TFMA, and 80.0 g of deionized water were transferred to the autoclave. Then, by double weighing, 10.0 g (0.10 mol) of VDF and 3.4 g (0.023 mol) of HFP were introduced to the mixture. Afterward, the autoclave was progressively heated to 80 °C by carrying out various plateaus at 50, 60, and 70 °C for 2 min. A small exotherm of ca. 5 °C was

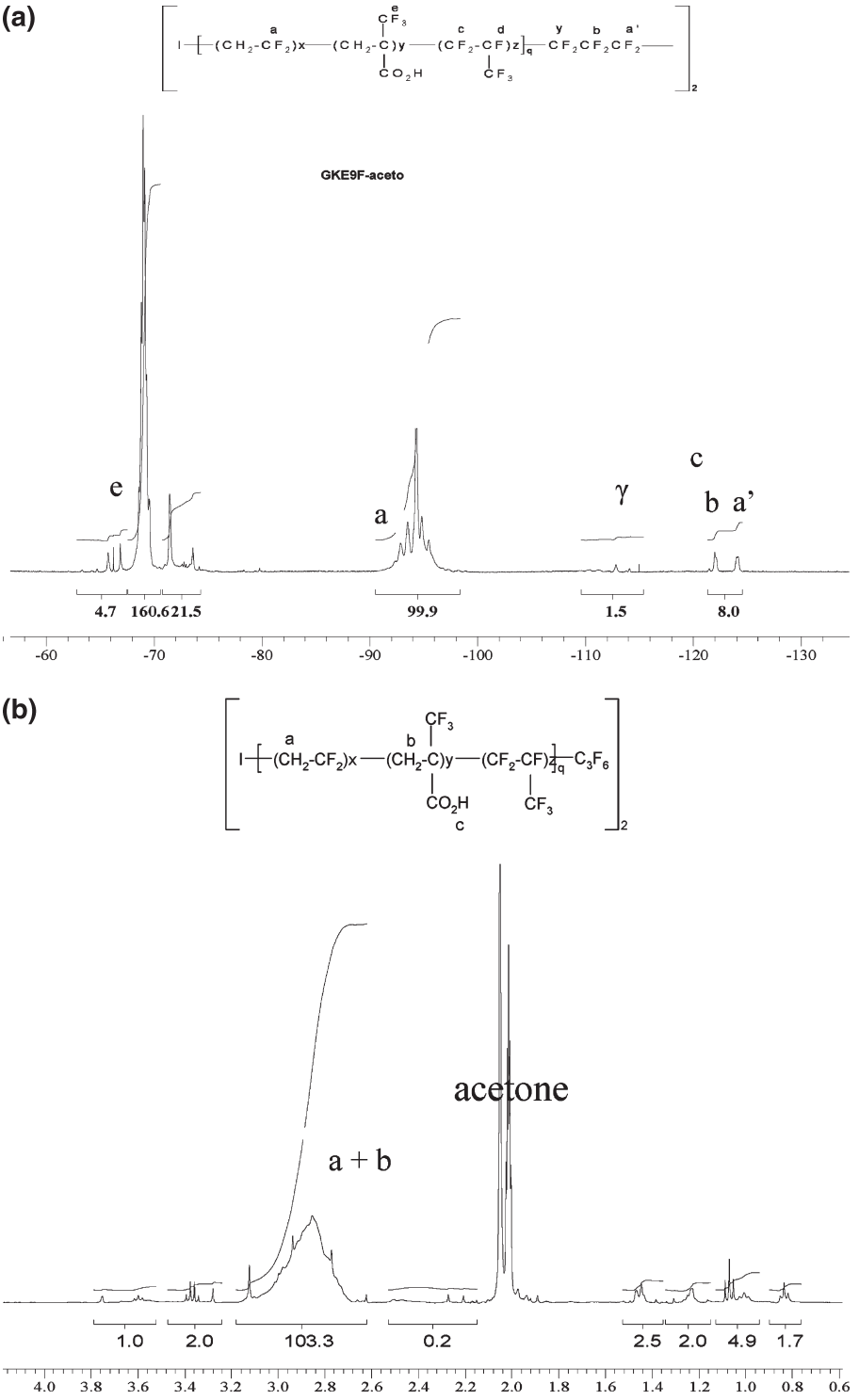

Figure 1. (a) Expansion of the −56 to −134 ppm zone of the ^{19}F NMR spectrum (registered in acetone-d_6) of poly(VDF-*ter*-TFMA-*ter*-HFP) terpolymer, synthesized in emulsion (run GKE9 in Table 1). Initial monomer molar ratio of VDF/TFMA/HFP 64/27/9; terpolymer composition of VDF/TFMA/HFP 49/53/7. (b) Expansion of the 0.6−4.2 ppm zone of the ^{1}H NMR spectrum (registered in acetone-d_6) of poly(VDF-*ter*-TFMA-*ter*-HFP) terpolymer, synthesized in emulsion (run GKE9 in Table 1). Initial monomer molar ratio of VDF/HFP/TFMA 64/27/9 mol %; terpolymer composition of VDF/TFMA/HFP 49/53/7 (VDF, TFMA, and HFP stand for vinylidene fluoride, α-trifluoromethacrylic acid, and hexafluoropropylene, respectively).

observed; then, a sharp drop of pressure to 10 bar occurred. After 6 h of reaction, the autoclave was placed in an ice bath for ~60 min, and 3 g of unreacted VDF and HFP were progressively released (conversion 78%). After opening the autoclave, about 100 g of latex miniemulsion was obtained. Water was removed by lyophilization (evaporation at −90 °C under 10 mbar). The TFMA was eliminated by precipitation from methanol to obtain a terpolymer (yield = 70−85%) as a white powder. The sample was characterized by ^{19}F and ^{1}H NMR spectroscopy and SEC analysis.

The poly(VDF-*ter*-TFMA-*ter*-HFP) terpolymers are soluble in polar solvents, such as acetone, DMF, dimethylacetamide, DMSO, NMP, THF, and methylethyl ketone.

Preparation of Poly(VDF-*ter*-TFMA-*ter*-HFP) Copolymers/Silica Gel Nanocomposites under Alkaline Conditions. To a methanol solution (4 mL) of poly(VDF-*ter*-TFMA-*ter*-HFP)

terpolymers [M_n = 5900 (0.20 g)] were added 0.10 mL of TEOS, and 30 wt % silica-nanoparticle methanol solution [0.67 g; average particle size: 11 nm (Methanol Silica-sol (TR)), and 25% aqueous ammonia solution (0.10 mL)]. The mixture was stirred with a magnetic stirring bar at room temperature for 2 h. After the solvent was evaporated off, 25 mL of methanol was added to the obtained crude products. The methanol solution was then stirred with a magnetic stirring bar at room temperature for 2 days and then was centrifuged for 30 min. The produced fluorinated nanocomposite was easily separated from the methanol solution. Fluorinated nanocomposite powders thus obtained were dried in vacuo at 50 °C for 2 days to afford purified particle powders (0.08 g).

Preparation of Poly(VDF-*ter*-TFMA-*ter*-HFP) Copolymers/Silica Gel Nanocomposites under Acidic Conditions. To a methanol solution (10 mL) of poly(VDF-*ter*-TFMA-*ter*-HFP) terpolymers [M_n = 5900 (0.10 g)] were added 0.25 mL of TEOS and 1 N HCl (0.38 mL). The mixture was stirred with a magnetic stirring bar at room temperature for 2 h. After the solvent was evaporated off, 13 mL of methanol was added to the obtained total product mixtures. The methanol solution was then stirred with a magnetic stirring bar at room temperature for 2 days and then was centrifuged for 30 min. The produced fluorinated nanocomposite was easily separated from the methanol solution. Fluorinated nanocomposite powders thus obtained were dried in vacuo at 50 °C for 2 days to afford purified particle powders (0.04 g).

Results and Discussion

The radical terpolymerization of VDF with TFMA and HFP was carried out in aqueous solution (initiated by $Na_2S_2O_8$ at 80 °C) in the presence of telechelic 1,6-diiodoperfluorohexane in water (Scheme 1) to obtain a stable emulsion. The polymer chain is composed of several VDF units (or even of oligo(VDF) blocks) separated by one TFMA unit due to the nonpropagation of TFMA[27,28] and random distribution of HFP.

At the end of the terpolymerization, the total product mixture was freeze-dried and then lyophilized to remove water. These products were precipitated from methanol and characterized by ^{1}H and ^{19}F NMR and by SEC.

Characterization of the Microstructure of Poly(VDF-*ter*-TFMA-*ter*-HFP) Terpolymers by NMR Spectroscopy. Figure 1a represents the ^{19}F NMR spectrum of the dried poly(VDF-*ter*-TFMA-*ter*-HFP) terpolymer produced from an initial $[VDF]_0/[TFMA]_0/[HFP]_0$ molar ratio of 62/29/9 and in the presence of $IC_6F_{12}I$ as the chain transfer agent (CTA). This spectrum shows the characteristic peak centered at −92 ppm (of small intensity) assigned to the difluoromethylene groups located in the head-to-tail VDF chaining (i.e., normal VDF addition, $-CH_2-CF_2-CH_2-CF_2$). The signals centered at −93.8 ppm (of high intensity) correspond to the difluoromethylene group of the VDF unit adjacent to a TFMA unit.[18,20] This arises from a microstructure of the terpolymer composed of poly(VDF-*alt*-TFMA) blocks separated by one HFP unit. Hence, it is noted the absence of signals centered at −113.4 and −115.7 ppm assigned to the CF_2 groups in $-CH_2-CF_2-CF_2-CH-$ and $-CH_2-CF_2-CF_2-CH_2-$ sequences, characteristic of the head-to-head addition of VDF adduct, which is also a clear evidence of the controlled of that terpolymerization, as reported in the ITP of VDF.[30,53,54] A broad peak at −68.1 ppm is attributed to the fluorine atoms in the $-CF_3$ group of TFMA incorporated in the copolymer,[18,20,49] whereas the signal of the monomer appears to be a single signal at −65.3 ppm. The characteristic signals of HFP units are centered at −72, −121, and −182 ppm assigned to CF_3, CF_2, and CF groups, respectively. The incorporation of difluoromethylene units in CTA is evidenced by the signals centered at −122, −124, and −112.2 ppm assigned to central $-(\underline{CF_2})_2-$ and $-(CF_2)_2-\underline{CF_2}-CH_2$ groups in CTA,[20,50,51] respectively, as useful labels to assess the numbers of VDF, HFP, and TFMA units (eqs 1−3).

Table 1. Molecular Characteristic Features of the Poly(VDF-*ter*-HFP-*ter*-TFMA) Terpolymers Utilized in this Study[a]

sample	M_n (g/mol) (assessed by ^{19}F NMR)	mol % of VDF	mol% of HFP	mol % of TFMA	PDI
GKB6	5400	80	8	12	1.4
GKE9	12 300	46	6	48	1.8
GKE15	5900	48	1	51	1.5

[a] M_n, PDI, VDF, TFMA, and HFP stand for average molecular weight in number, polydispersity index, vinylidene fluoride, α-trifluoromethacrylic acid, and hexafluoropropylene, respectively.

The characteristic end groups of the terpolymers terminated by a VDF unit appear at −40.0 and −108.0 ppm, which are assigned to $-CH_2CF_2I$ and $-CF_2CH_2I$, respectively. The presence of two different end groups was explained by the special ability of VDF to undergo the addition of a macroradical onto the CH_2═ site (normal addition, major proportion (95 mol %), yielding head-to-tail addition) but also onto the CF_2═ one (reverse addition, minor proportion (5 mol %), yielding head-to-head addition). It is worth noting that the sum of $-CF_2I$ and $-CH_2I$ (termination by a VDF unit) corresponds to total end chains. This proves the absence of end chain terminated by a TFMA unit ($-C(CF_3, CO_2H)-I$) or by (HFP)I because $CF_2CF(CF_3)I$ and $CF_2-CFICF_3$ should lead to signal centered at −60 and −145 ppm, respectively (Figure 1a).[52] Both the weak stability of the C−I bond and the steric hindrance from the presence of both CF_3 and CO_2H groups support this hypothesis. Moreover, the absence of the $-CF_2-I$ end group for high-molecular-weight material was observed (Table 1). This result can also be explained by the difference of reactivity between $-CF_2I$ and $-CH_2I$ species, as noted in previous works on the ITP of VDF.[20,24,53,54] Thus, $-CF_2I$ species is more reactive than $-CH_2I$, which explains the accumulation of $-CH_2I$ in the course of the copolymerization. In conclusion, the suggested decreasing order of reactivity is as follows: $-C(CF_3)-I > -CF_2-I > -CH_2-I$.

Examination of the ^{19}F NMR spectra allowed us to assess the $DP_{n,experimental,VDF}$ (i.e., the number of VDF units), that of TFMA, $DP_{n,experimental,TFMA}$ (i.e., the number of TFMA units), and HFP, $DP_{n,experimental,HFP}$ (i.e., the number of HFP units) in the terpolymer from eqs 1−3.

$$DP_{n,VDF} = \left(\int CF_2{}^{at-40.0ppm} + \int CF_2{}^{at-92ppm} + \int CF_2{}^{at-93.8ppm} + \int CF_2{}^{at-108.0ppm}\right) / 2 / \left(\left[\left(\int C_4F_8{}^{from-122\ to-124\ ppm} - 2\times\int CF_3{}^{from-72.0}/3\right)\right]8\right) \quad (1)$$

$$DP_{n,TFMA} = \left(\int CF_3{}^{at-68.1ppm}/3\right) / \left(\left[\left(\int C_4F_8{}^{from-122\ to-124\ ppm} - 2\times\int CF_3{}^{from-72.0}/3\right)\right]/8\right) \quad (2)$$

$$DP_{n,HFP} = \left(\int CF_3{}^{from-70\ to-75\ ppm}/3\right) / \left(\left[\left(\int C_4F_8{}^{from\ -122\ to\ -\ 124\ ppm} - 2\times\int CF_3{}^{from-70\ to-75\ ppm}/3\right)\right]/8\right) \quad (3)$$

where ($\int CF_x^{at-i ppm}$ represents the integral of the signal centered at $-i$ ppm assigned to CF_x ($x = 2$ or 3).

For example, from run GKE-15 (Table 1), eqs 1−3 indicate that poly(VDF-*ter*-HFP-*ter*-TFMA) terpolymer is composed of 25 VDF, 0.5 HFP, and 26.5 TFMA units, hence leading to an average molecular weight, $M_n = 5900$.

The ^{1}H NMR spectrum (Figure 1b) confirms the terpolymerization of TFMA by the absence of signals at 6.5 and at 6.7 ppm assigned to the methylene group of the double bond ($C\underline{H_2}$=) of TFMA monomer. The spectrum also shows different multiplet and triplet centered in the 2.7 to 3.1 ppm range and 3.6 ppm attributed to $-\underline{CH_2}-$ of VDF and TFMA and to $-CF_2C\underline{H_2}-I$, respectively. The absence of the triplet of triplets centered at 6.3 ppm, assigned to HCF_2CH_2, is evidence that there is no observable transfer to water, to the monomers, or to the copolymer. The absence of signal centered in the 2.3 to 2.5 ppm range attests the absence of tail-to-tail addition of VDF (i.e., $-CF_2-C\underline{H_2}-C\underline{H_2}-CF_2-$), which is also an evidence of the controlled behavior of the terpolymerization, as noted for the iodine transfer homopolymerization of VDF[53,54] in the iodine transfer copolymerizations of VDF with perfluoromethyl vinyl ether,[51] or with TFMA,[20] and the iodine transfer terpolymerization of VDF with HFP and pentafluorosulfonyle monomers.[24]

The presence of end group, such as $-CF_2I$ or $-CH_2I$, can be exploited to incorporate a range of chemical functionalities, such as alcohol, carboxylic acid, azido, ester, and allylic functions[4,16,17] or to synthesize block polymers.[17] However, $-CH_2I$ end group is less reactive[54] and cannot easily react onto another monomer (to lead to block copolymer), and its modification under nucleophilic substitution should induce some dehydrofluorination of VDF units in VDF-HFP dyads.[4,17]

The $-CF_2I$ amount in the poly(VDF-*ter*-HFP-*ter*-TFMA) terpolymer decreases with the number of VDF units inserted in the polymer chain. This result was also observed in the case of the homopolymerization of VDF,[53,54] the copolymerizations of VDF with perfluoromethyl vinyl ether[51] or with TFMA,[20] and the terpolymerization of VDF with HFP and pentafluorosulfonyle monomers.[24] This can be explained by the inversion of VDF during the polymerization and the difference of reactivity between $-CH_2I$ and $-CF_2I$ end groups shown by their transfer constants ($C_{tr} = 7.7$ and 0.3, respectively at 75 °C).[54]

The comparison of different polymerizations, that is, the homopolymerization of VDF,[50] the copolymerization of VDF and TFMA,[20] and the terpolymerization of VDF with HFP and 1,1,2-trifluoro-2-pentafluorosulfanylethylene,[24] exhibits a similar trend on the evolution of $-CF_2I$ functionality versus the number of VDF units. However, the terpolymer induced a less significant decrease. Presently, the explanation is not clear, but it is possible to claim that the insertion of HFP- and SF_5-containing monomers[24] can limit the inversion of VDF by the electronic effect or by the steric hindrance of their CF_3 and SF_5 side groups.

When the feed VDF percentage is higher than 75 mol %, the incorporation of VDF in the copolymer was always higher than that in the initial composition. This showed that TFMA and HFP are less reactive than VDF, as evidenced by their reactivity ratios, $r_{TFMA} = 0$ and $r_{VDF} = 1.6$[18,20] and $r_{HFP} = 0$ and $r_{VDF} = 3$ to 5[17] at 80 °C. However, as noted in a previous work,[18] when feed VDF percentage is lower than 70 mol %, an alternating tendency of VDF and MTFA is observed, hence leading to a random microstructure where poly(VDF-*alt*-TFMA) alternated blocks are separated by one HFP unit.

2. Assessment of the Molecular Weights of Poly(VDF-*ter*-TFMA-*ter*-HFP)-I Terpolymers. As expected for the ITP,[29] the polydispersity indices (PDIs) are close to 1.4 to 1.8 and indicate a certain control of the radical polymerization.[30]

The molecular weights of the copolymers can also be tuned by varying the CTA concentration. The targeted molecular weights were determined from eq 4. Table 1 shows that these values are in good agreement with experimental ones assessed by NMR (from average degree of polymerization assessed from eqs 1−3).

$$M_{n,\,targeted} = ([VDF]_0 \times M^{VDF} + [TFMA]_0 \times M^{TFMA} + [HFP]_0 \times M^{HFP})/([CTA]_0) + M^{CTA} \quad (4)$$

where [*i*], M^{TFMA}, M^{VDF}, M^{HFP}, and M^{CTA} stand for the number of *i* base units and the molar masses of TFMA (140 g·mol^{-1}), VDF (64 g·mol^{-1}), HFP (150 g·mol^{-1}), and CTA (554 g·mol^{-1}), respectively.

In addition, the SEC results show a good correlation with the molecular weights assessed by NMR, and as mentioned above, a low PDI (1.4 to 1.8).

As expected,[18,20] the increase in the TFMA concentration in the feed ratio favored an increase in the TFMA monomer in the copolymers.

Preparation of Poly(VDF-*ter*-TFMA-*ter*-HFP) Terpolymers/Silica Gel Nanocomposites. Poly(VDF-*ter*-TFMA-*ter*-HFP) terpolymers exhibit a good solubility in water and polar organic solvents such as methanol, ethanol, dimethyl formamide, dimethyl acetamide, and tetrahydrofuran. They also exhibit a stimuli thermoresponsive behavior because poly(VDF-*ter*-TFMA-*ter*-HFP) terpolymers disassembled upon heating above 50 °C and reassembled upon cooling.[45] Furthermore, they may be regarded as novel fluorinated polysoaps, which can form self-assembled fluorinated aggregates in these solvents.[46,48] The size of fluorinated polymeric aggregates was assessed in methanol by the DLS measurements at 25 °C, and the size of the aggregates was found to be nanometer-size-controlled (76 ± 8 nm). ABA triblock-type fluorinated polysoaps such as fluoroalkyl end-capped acrylic acid oligomer [R_F-$(CH_2CHCOOH)_n$-R_F; R_F = fluoroalkyl groups] were previously reported to form similarly nanometer-size-controlled molecular aggregates in aqueous and organic media.[46,48]

In addition, these fluorinated oligomers were applied to the preparation of fluorinated oligomers/silica nanocomposites that can exhibit interesting characteristics imparted by both fluorine and silica nanoparticles.[48] Actually, many hydrogenated polymers mixed with TEOS and cross-linked via a sol−gel process led to hydrogenated polymers/silica composites and were recently reviewed.[55] Hence, for the first time, novel poly(VDF-*ter*-TFMA-*ter*-HFP) terpolymers/silica nanocomposites were prepared by sol−gel reactions of the corresponding fluorinated terpolymer with TEOS and silica nanoparticles in methanol under alkaline and acidic conditions, respectively. These results are displayed in Scheme 2.

Hence, poly(VDF-*ter*-TFMA-*ter*-HFP) terpolymers/silica composites were produced in 17−24% isolated yields under alkaline or acidic conditions. These fluorinated silica composites thus obtained were found to exhibit good dispersibility and stability not only in water but also in methanol, ethanol, and tetrahydrofuran. The size of these fluorinated composites in methanol was assessed by DLS at 25 °C. These composites are nanometer-size-controlled (24−137 ± 2−23 nm) fine particles. The size of each composite was found to increase effectively by the nanocomposite reactions compared with the parent silica nanoparticles (11 nm), indicating that core (silica nanoparticle)/corona (fluorinated copolymer)-type nanoparticles should be smoothly produced by sol−gel reactions (Scheme 2). In particular, fluorinated terpolymer should be incorporated homogeneously into the silica gel nanoparticles that include the hydrolyzate of TEOS, utilizing hydrogen-bonding interaction

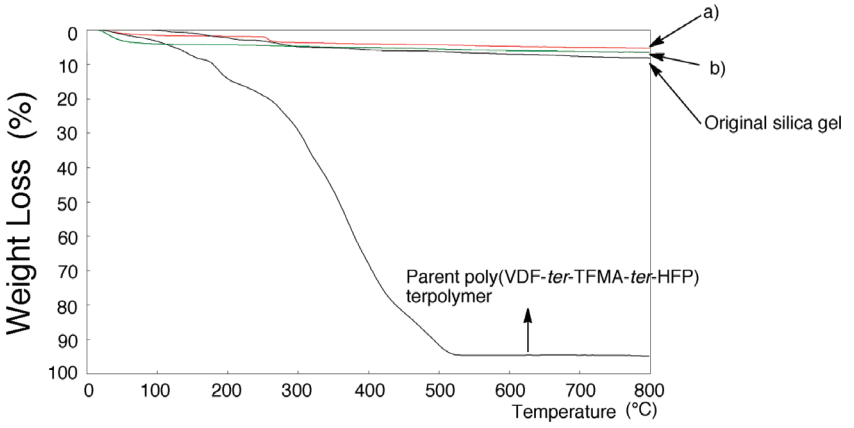

Figure 2. TGA thermograms under air of silica gel, parent poly(VDF-*ter*-TFMA-*ter*-HFP) terpolymer (M_n = 5900 g·mol^{-1}), and poly(VDF-*ter*-TFMA-*ter*-HFP) terpolymer/SiO_2 nanocomposites, the size of which are (a) 37.0 nm (run 2, Scheme 2) and (b) 23.7 nm (run 1, Scheme 2) achieved by alkaline sol gel procedure (where VDF, TFMA, and HFP stand for vinylidene fluoride, α-trifluoromethacrylic acid, and hexafluoropropylene, respectively).

Scheme 2. Preparation of Poly(VDF-*ter*-TFMA-*ter*-HFP) Terpolymer/Silica Nanocomposites

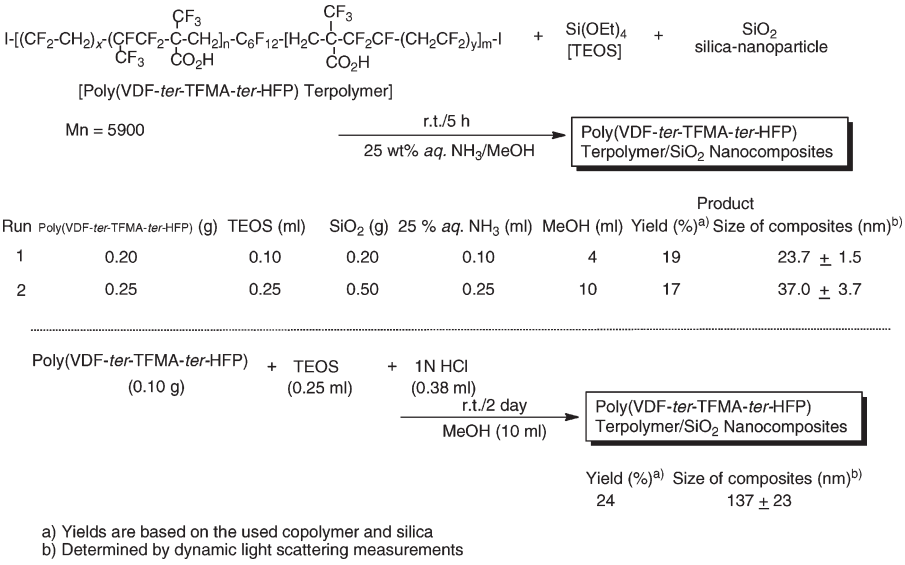

Run	Poly(VDF-*ter*-TFMA-*ter*-HFP) (g)	TEOS (ml)	SiO_2 (g)	25 % *aq.* NH_3 (ml)	MeOH (ml)	Product Yield (%)[a]	Size of composites (nm)[b]
1	0.20	0.10	0.20	0.10	4	19	23.7 ± 1.5
2	0.25	0.25	0.50	0.25	10	17	37.0 ± 3.7

Yield (%)[a]	Size of composites (nm)[b]
24	137 ± 23

a) Yields are based on the used copolymer and silica
b) Determined by dynamic light scattering measurements

Scheme 3. Schematic Illustration of Poly(VDF-*ter*-TFMA-*ter*-HFP) Terpolymer/Silica Nanocomposites

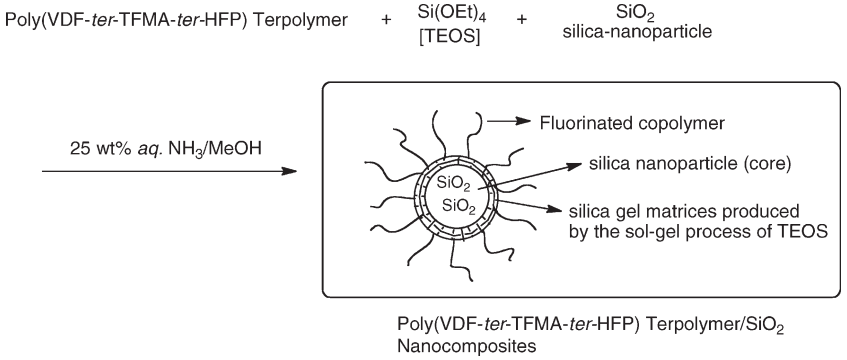

between the silanol groups and carboxyl groups of terpolymer to afford expected fluorinated terpolymer/silica nanocomposites depicted in Scheme 3.

The thermal properties of these new poly(VDF-*ter*-TFMA-*ter*-HFP) terpolymers/silica nanocomposites were investigated by thermogravimetric analyses (TGA) under air. The weight loss of these nanocomposites was measured by increasing the temperatures to ~800 °C at a heating rate of 10 °C/min. Figures 2 and 3 display the thermograms of the poly(VDF-*ter*-TFMA-*ter*-HFP) terpolymers and of the poly(VDF-*ter*-TFMA-*ter*-HFP) terpolymers/silica nanocomposites achieved under either alkaline (Figure 2) or acidic (Figures 3) conditions, respectively.

The weight of parent poly(VDF-*ter*-TFMA-*ter*-HFP) terpolymers markedly dropped around 255 °C and decomposed completely at ca. 500 °C. First, a decarboxylation of MTFA units occurred, followed by the dehydrofluorination of VDF-HFP dyads. A similar tendency was observed in poly(VDF-*ter*-TFMA-*ter*-HFP) terpolymer/silica nanocomposite, which was prepared under acidic conditions, and a quasi-constant value for its weight loss was observed above 500 °C. Differential thermal analyses (DTA) (Figure 4) of this nanocomposite in air atmosphere (heating rate: 10 °C/min) showed that as the temperature reached ~350 °C, exothermic phenomenon occurred, and a sharp exothermic peak was noted around 490 °C, which arises from the complete decomposition of poly(VDF-*ter*-TFMA-*ter*-HFP) terpolymers in the nanocomposite.

Poly(VDF-*ter*-TFMA-*ter*-HFP) terpolymer/silica nanocomposites, which were prepared under alkaline conditions, were unexpectedly found to exhibit almost no weight loss even after calcination at 800 °C as well as that of the original silica gel (Figure 2). Additionally, DTA measurements did not show any clear exothermic peak for these nanocomposites (Figure 4b). This result may arise from the exceptional thermal stability of these nanocomposites, even at 800 °C.

To clarify the surface morphology of these nanocomposites, we measured the mean zeta potential of well-dispersed aqueous solutions based on poly(VDF-*ter*-TFMA-*ter*-HFP) terpolymer/silica nanocomposites that do not show any weight loss (run 1, Scheme 2), and the results are supplied in Table 2.

The mean zeta potential of poly(VDF-*ter*-TFMA-*ter*-HFP) terpolymers/silica nanocomposite (run 1, Scheme 2) before calcination had a negatively enhanced charge (−20.9 mV) compared with that of the original silica nanoparticle (−11.7 mV, Table 2), indicating that negatively charged carboxyl groups in fluorinated copolymer should be arranged on the composite particle surface through the nanocomposite reactions in Scheme 2. A similar negatively enhanced charge (−18.4 mV) was obtained in poly(VDF-*ter*-TFMA-*ter*-HFP) terpolymers/silica nanocomposite that possess a clear weight loss behavior. The decrease in the negatively charged values from −20.9 to −14.1 mV in the calcinated nanocomposites demonstrates that the carboxyl groups onto the particle surfaces can be partially consumed all along the calcination process. These results suggest that a certain core/corona (silica nanoparticle/fluorinated copolymer containing carboxyl groups)-type nanoparticles could be smoothly prepared by the sol−gel reactions mentioned in Table 3.

The field-emission scanning electron micrograph (FE-SEM) of poly(VDF-*ter*-TFMA-*ter*-HFP) terpolymer/silica nanocomposite (runs 1 and 2 in Table 3) before and after

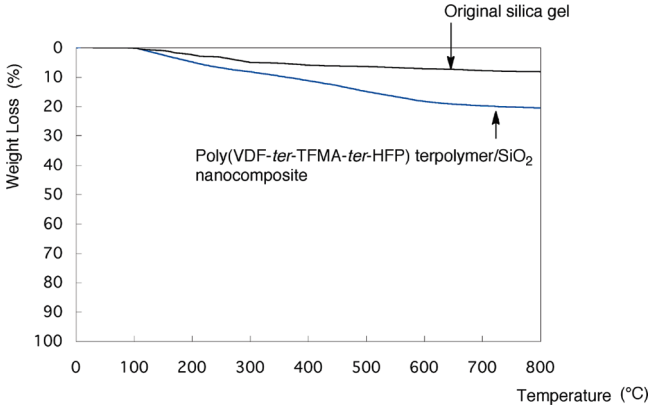

Figure 3. TGA thermograms of various poly(VDF-*ter*-TFMA-*ter*-HFP) terpolymers/silica nanocomposites obtained by acidic sol gel procedure (Scheme 2) under air compared with silica gel (where VDF, TFMA, and HFP stand for vinylidene fluoride, α-trifluoromethacrylic acid, and hexafluoropropylene, respectively).

Table 2. Particle Size and Zeta Potential of Poly(VDF-*ter*-TFMA-*ter*-HFP) Terpolymers/Silica Nanocomposite before and after Calcinations

composites	particle size (nm)	zeta potential (mV)
before calcination	24[a]	−20.9
after calcination	50[a]	−14.1
original silica nanoparticle	11	−11.7

[a] Determined by dynamic light scattering measurements (where VDF, TFMA, and HFP stand for vinylidene fluoride, α-trifluoromethacrylic acid, and hexafluoropropylene, respectively).

Table 3. Mean Diameter (Assessed by Field-Emission Scanning Electron Micrograph, FE-SEM) of Poly(VDF-*ter*-TFMA-*ter*-HFP) Terpolymer/Nanocomposites before and after Calcinations

	mean diameter (nm)	
	before calcination	after calcination
run 1	53	20
run 2	17	24

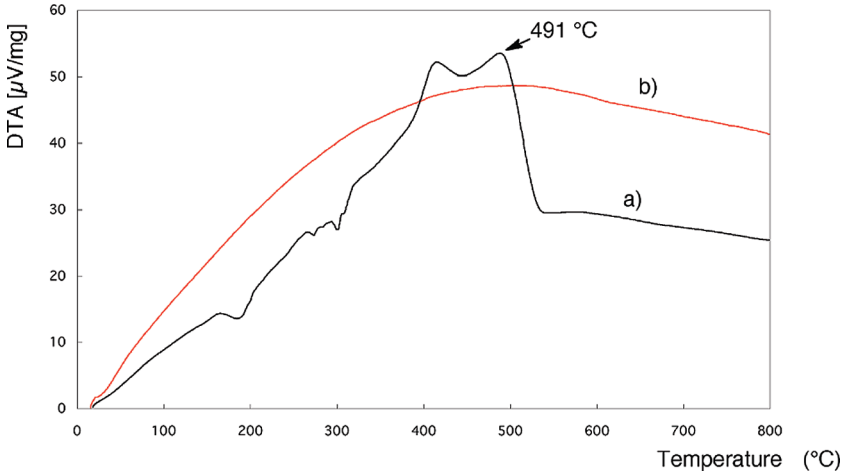

Figure 4. Differential thermal analyses of poly(VDF-*ter*-TFMA-*ter*-HFP) terpolymer/SiO_2 nanocomposites: (a) weight loss for nanocomposites synthesized from acidic sol gel conditions and (b) no weight loss for nanocomposites synthesized from alkali sol gel conditions (run 1, Scheme 2).

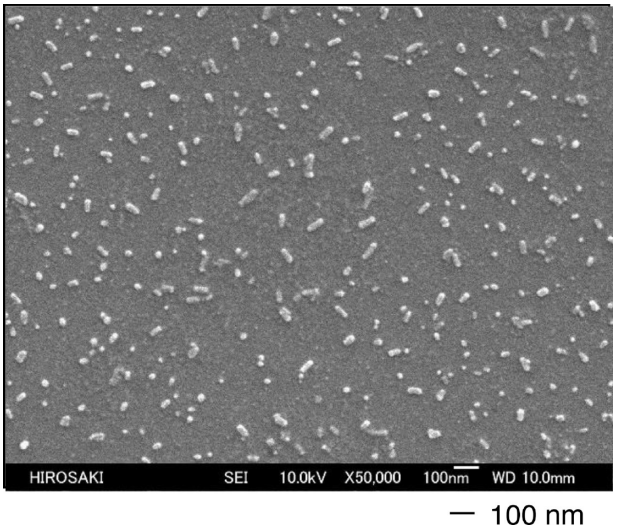

Figure 5. FE-SEM (field-emission scanning electron microscopy) image of poly(VDF-*ter*-TFMA-*ter*-HFP) terpolymer/SiO_2 nanocomposite (run 1 in Scheme 2) before calcination at 800 °C.

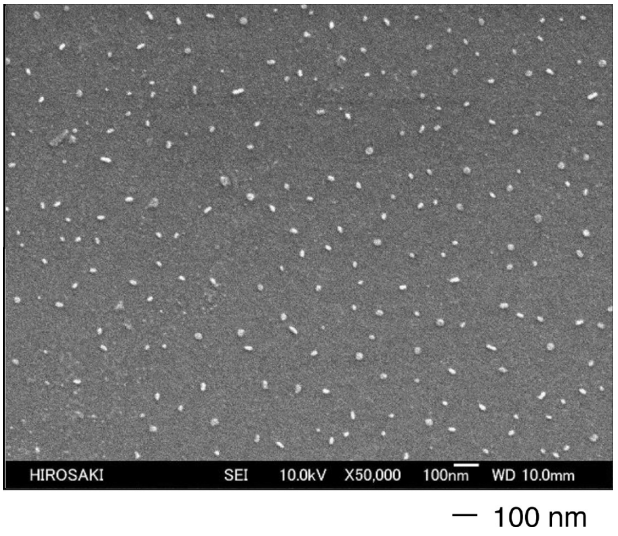

Figure 6. FE-SEM (field-emission scanning electron microscopy) image of poly(VDF-*ter*-TFMA-*ter*-HFP) terpolymer/SiO_2 nanocomposite (run 1 in Scheme 2) after calcination at 800 °C.

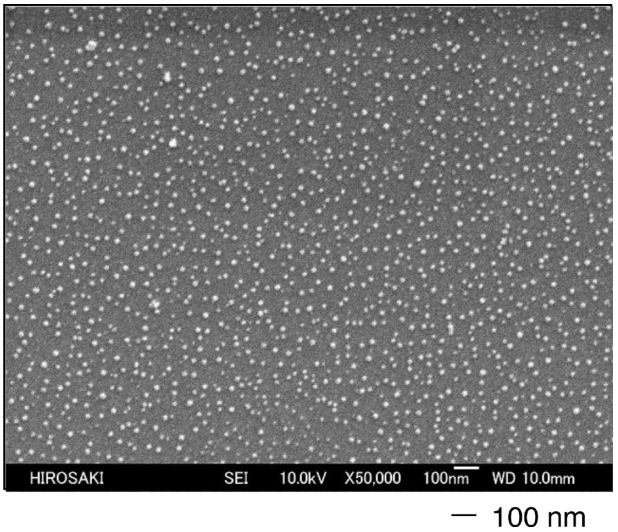

Figure 7. FE-SEM (field-emission scanning electron microscopy) image of poly(VDF-*ter*-TFMA-*ter*-HFP) terpolymer/SiO_2 nanocomposite (run 2 in Scheme 2) before calcination at 800 °C.

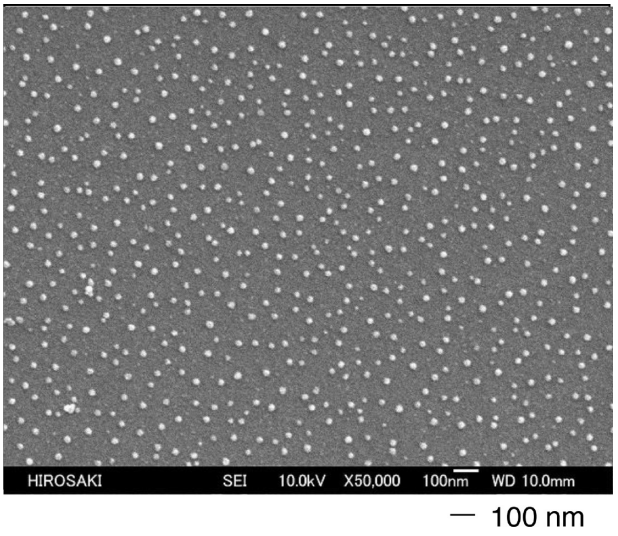

Figure 8. FE-SEM (field-emission scanning electron microscopy) image of poly(VDF-*ter*-TFMA-*ter*-HFP) terpolymer/SiO_2 nanocomposite (run 2 in Scheme 2) after calcination at 800 °C.

calcination showed the formation of fine particles, respectively, and the mean diameter of these nanocomposite particles is listed in Table 3 (from Figures 5−8).

Interestingly, the similar particle sizes were observed before and after calcinations (Figures 5−8). In addition, it was noted that the white color of all nanocomposite powders did not change before and after calcination at 800 °C.

To confirm the absence of weight loss, we characterized calcinated poly(VDF-*ter*-TFMA-*ter*-HFP) terpolymer/silica nanocomposites prepared under alkaline (Run 1, Scheme 2) and acidic conditions (Run 3, Scheme 2) by ^{19}F MAS NMR spectroscopy (Figure 9).

The ^{19}F MAS NMR spectrum of each poly(VDF-*ter*-TFMA-*ter*-HFP) terpolymer/silica nanocomposite before calcination exhibits the characteristic signals centered between −50 and −80 ppm and in the −100 to −130 ppm range, assigned to CF_3 and to CF_2 groups, respectively, as evidence of the presence of the fluorinated terpolymer in the nanocomposites. However, when the nanocomposite was prepared under alkaline conditions, a relatively clear signal was unexpectedly noted at ca. −190 ppm. That signal would be ascribed to the presence of hexafluorosilicate derivatives, but Zeng and Stebbins[56] and Kao and Chen[57] reported that ^{19}F MAS NMR chemical shifts of sodium hexafluorosilicate and ammonium hexafluorosilicate are centered at −152 and −158 ppm, respectively. Thus, in this present study, the signal centered at −190 ppm seems different from these above ones. Nevertheless, the ^{19}F NMR spectrum of C_4F_9-$[CF_2CF(CF_3)](CH_2CF_2)I$[58] exhibits a signal centered at −184 ppm assigned to the CF group of the HFP unit.[58] However, the HFP content that induces the presence of a signal assigned to CF in poly(VDF-*ter*-TFMA-*ter*-HFP) terpolymer (GKE15 in Table 1) is quite low (1 mol %) and is even negligible in the ^{19}F MAS NMR spectrum of the virgin poly(VDF-*ter*-TFMA-*ter*-HFP) terpolymer before calcination. Therefore, the chemical shift present at −190 ppm cannot be attributed to CF in polymers. In fact, it might be assumed that iodine atoms in I-$[(VDF)_x$-HFP-TFMA$]_n$-C_6F_{12}-[TFMA-HFP-$(VDF)_y]_m$-I could react with ammonium hexafluorosilicate through anion exchange reactions

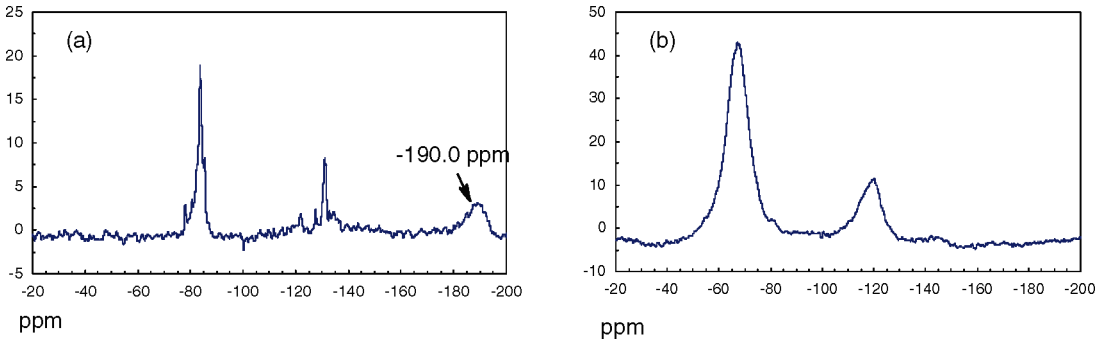

Figure 9. ^{19}F MAS NMR spectra of poly(VDF-*ter*-TFMA-*ter*-HFP) terpolymer/SiO_2 nanocomposites possessing (a) no weight loss characteristic and (b) weight loss characteristic before calcination at 800 °C determined by 3.2 mm ^{19}F MAS probe.

Scheme 4. Plausible Mechanism for the Formation of Ammonium Hexafluorosilicate

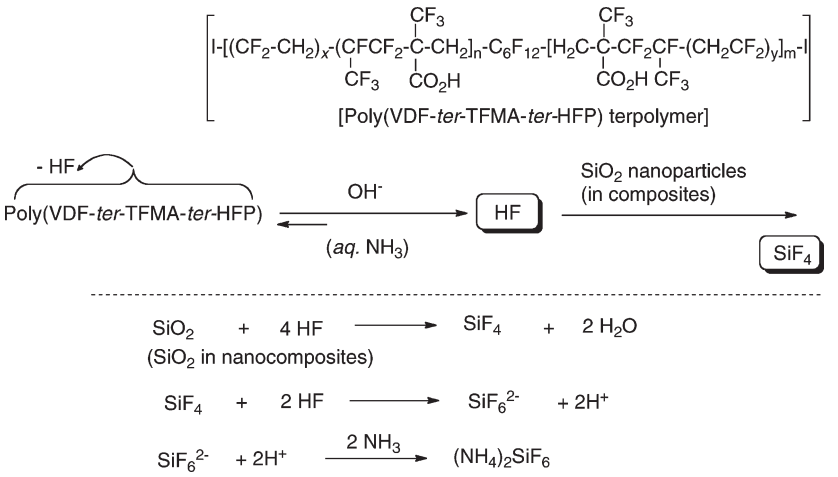

to lead to $[[(VDF)_x\text{-HFP-TFMA}]_n\text{-}C_6F_{12}\text{-}[\text{TFMA-HFP-}(VDF)_y]_m]SiF_6$ and ammonium iodide. This hexafluorosilicate derivative could afford signals at around −190 ppm in the ^{19}F MAS NMR. This observation may explain that the nanocomposites generated from poly(VDF-*ter*-TFMA-*ter*-HFP) terpolymers with silica nanoparticles should proceed smoothly under alkaline conditions to yield not only the expected poly(VDF-*ter*-TFMA-*ter*-HFP) terpolymer/silica nanocomposites but also ammonium hexafluorosilicate, as shown in the suggested reaction mechanism (Scheme 4). This observation may occur because these terpolymers based on VDF should undergo a possible dehydrofluorination under such basic conditions[15−17] in the presence of silica nanoparticles as the cocatalyst (Scheme 4).

The formation of ammonium hexafluorosilicate during the composite reactions can afford no weight-loss characteristic of poly(VDF-*ter*-TFMA-*ter*-HFP) terpolymer. This means that such fluorinated terpolymers involved in the preparation of nanocomposites should effectively be encapsulated (or confined) to the nanometer-size-controlled silica gel matrices through a molecular-level synergistical combination. This arises from not only the strong interactions between fluorine atoms in the copolymer and silicon atoms in silica gel nanocomposite but also the efficient interactions between hexafluorosilicic acid and poly(VDF-*ter*-TFMA-*ter*-HFP) terpolymers in silica gel matrices to afford such a high thermal stability of these resulting nanocomposites in the calcination process.

Fluoroalkyl end-capped oligomer-containing carboxyl groups, such as $[R_F\text{-}(CH_2CHCOOH)_n\text{-}R_F]$/silica nanocomposites, have already been reported to favor a clear weight loss at 800 °C corresponding to the contents of oligomer in the composites.[59] Similarly, fluoroalkyl end-capped methacrylic acid oligomer $[R_F\text{-}(CH_2CMeCOOH)_n\text{-}R_F]$/silica nanocomposites can exhibit a clear weight loss behavior under similar conditions.[60] $R_F\text{-}(CH_2CMeCOOH)_n\text{-}(CH_2\text{-}CCF_3COOH)_n\text{-}R_F$ cooligomer can possess a higher acidic carboxyl groups as well as poly(VDF-*ter*-TFMA-*ter*-HFP) terpolymer because of the presence of electron-withdrawing CF_3 groups in the cooligomer compared with that of $R_F\text{-}(CH_2CHCOOH)_n\text{-}R_F$ or $R_F\text{-}(CH_2CMeCOOH)_n\text{-}R_F$ oligomers. Therefore, the resulting composite achieved from this fluorinated cooligomer is expected to give almost no weight loss at 800 °C, similarly to those obtained from poly(VDF-*ter*-TFMA-*ter*-HFP) terpolymers.[60]

In this way, the present interesting result of exceptional thermal stability of poly(VDF-*ter*-TFMA-*ter*-HFP) terpolymer/silica nanocomposites would be due to the higher acidity of carboxyl groups possessing electron-withdrawing CF_3 units as neighboring groups in these terpolymers. Hence, these higher acidic carboxyl groups of poly(VDF-*ter*-TFMA-*ter*-HFP) terpolymers should enable us to proceed to smooth dehydrofluorination of the carboxyl protons with fluorine atoms in the copolymer catalyzed by ammonia and silica nanoparticles to afford ammonium hexafluorosilicate suggested in Scheme 4. In contrast, no dehydrofluorination should afford a usual weight loss behavior in fluorinated copolymer/silica composites.

Conclusions

Iodine transfer terpolymerization of TFMA, VDF, and HFP led to terpolymers in high yields in aqueous medium in the

absence of any surfactants and in the presence of 1,6-diiodoperfluorohexane as the chain transfer agent. A first part showed that VDF, HFP, and TFMA can be terpolymerized by ITP, leading to relevant microstructures of resulting poly(VDF-*ter*-TFMA-*ter*-HFP) terpolymers composed of poly(VDF-*alt*-TFMA) alternated copolymeric blocks separated by one HFP unit. Interestingly, the introduction of TFMA in the emulsion of VDF allows us to improve the control and the process of the polymerization without adding any surfactant. Although the linear "molar masses - comonomer conversions" relationship was not supplied, the good agreement between the theoretical and experimental molecular weights was demonstrated, and the controlled character of that terpolymerization was enhanced by the narrow PDI values and the absence of reversed VDF-VDF dyads. Poly(VDF-*ter*-TFMA-*ter*-HFP) terpolymers were involved in the preparation of fluorinated copolymer/silica nanocomposites under alkaline and acidic conditions. According to the experimental conditions, various features of the nanocomposites were observed in terms of size (the acidic procedure led to bigger average-diameter nanocomposites) and thermal stability. The fluorinated nanocomposites, prepared under alkaline conditions, were interestingly found to exhibit almost no weight loss behavior at 800 °C (because of the formation of hexafluorosilicate), although those synthesized under acidic conditions exhibited a clear weight-loss behavior. Further surveys on the potential applications as fuel cell membranes,[61] surfactants, or paints and coatings are under progress.

Acknowledgment. We thank the Solvay S.A. (Tavaux, France and Brussels, Belgium) and Tosoh F-Tech Company (Shunan, Japan, Drs. Yoshida and Kawada) for providing VDF and TFMA comonomers, respectively, and CNRS and ARPE programme for financial support. The Bulgarian Ministry of Education and Science (National Science Fund) is also acknowledged for G.K.'s support.

References and Notes

(1) Feiring, A. E. In *Organofluorine Chemistry: Principles and Commercial Applications*; Banks, R. E., Smart, B. E., Tatlow, J. C., Eds.; Plenum Press: New York, 1994; Vol. *15*, pp 339−372.
(2) Scheirs, J. *Modern Fluoropolymers*; Wiley: New York, 1997.
(3) Hougham, G.; Cassidy, P. E.; Johns, K.; Davidson, T., *Fluoropolymers 2: Properties*; Kluwer/Plenum: New York, 1999.
(4) Ameduri, B.; Boutevin, B. *Well-Architectured Fluoropolymers: Synthesis, Properties and Applications*; Elsevier: Amsterdam, 2004.
(5) Banks, B. A. In *Modern Fluoropolymers*; Scheirs, J., Ed.; Wiley and Sons: New York, 1999; Chapter 4, pp 103−114.
(6) Pawloski, A. R.; La Fontaine, B.; Levinson, H. J.; Hirscher, S.; Schwarzl, S.; Lowack, K.; Kamm, F.-M.; Bender, M.; Domke, W.-D.; Holfeld, C.; Dersch, U.; Naulleau, P.; Letzkus, F.; Butschke *Proc. SPIE* **2004**, *5567*, 762.
(7) (a) Liu, W.; Koike, Y.; Okamoto, Y. *Macromolecules* **2005**, *38*, 9466–9473. (b) Mikes, F.; Yang, Y.; Teraoka, I.; Ishigure, T.; Koike, Y.; Okamoto, Y. *Macromolecules* **2005**, *38*, 4237–4245. (c) Mikes, F.; Teng, H.; Kostov, K.; Ameduri, B.; Koike, Y.; Okamoto, Y. *J. Polym. Sci., Part A: Polym. Chem.* **2009**, *47*, 6571–6578.
(8) (a) Iacono, S. T.; Budy, S. M.; Jin, J.; Smith, D. W., Jr. *Macromolecules* **2007**, *45*, 5705–5721. (b) Ligon, S. C.; Ameduri, B; Boutevin, B.; Smith, D. W. *Polym. Bull.* **2008**, *60*, 343–349.
(9) Boutevin, B.; Pietrasanta, Y. *Les Acrylates et Polyacrylates Fluorés*; Erec: Paris, 1989.
(10) Dams, R. J.; Martin, S. J. (3M company). U.S. Patent 2005/121,644, 2005.
(11) (a) Robinson, D.; Seiler, D. A. Potential Applications For Kynar Flex PVDF in the Nuclear Industry. In *Proceedings American Glovebox Society, National Conference, Linings, Coatings, and Materials*, Seattle WA, August 16, 1993; pp 10−14.
(12) Bongiovanni, R.; Malucelli, G.; Pollicino, A.; Tonelli, C.; Simeone, G.; Priola, A. *Macromol. Chem. Phys.* **1998**, *199*, 1099.
(13) (a) Wang, P.; Zakeerudin, S. M.; Grätzel, M. *J. Fluorine Chem.* **2004**, *125*, 1241–1253. (b) Zhang, J. H.; Han, H.; Xu, S.; Wu, S.; Zhou, C.; Yang, Y.; Zhao, X. *J. Appl. Polym. Sci.* **2008**, *109*, 1369.
(14) (a) Sha, J.; Ober, C. K. *Polym. Int.* **2009**, *58*, 302–306. (b) Losurdo, M.; Giangregorio, M. M.; Capezzuto, P.; Cardone, A.; Martinelli, C.; Farinola, G. M.; Babudri, F.; Naso, F.; Bruno, G. *Adv. Mater.* **2009**, *21*, 1–6.
(15) Seiler, D. A. PVDF in the Chemical Process Industry. In *Modern Fluoropolymers*; Scheirs, J. E., Ed.; Wiley: New York, 1997; pp 487−506.
(16) Humphrey, J. S.; Amin-Sanayei, R. Vinylidene Fluoride Polymers. In *Encyclopedia of Polymer Science and Technology*, 3rd ed.; Mark, H. F., Ed.; Wiley: New York, 2004; Vol. *4*, pp 510−533.
(17) Ameduri, B. *Chem. Rev.* **2009**, *109*, 6632–6686.
(18) Souzy, R.; Ameduri, B.; Boutevin, B. *Macromol. Chem. Phys.* **2004**, *205*, 476–485.
(19) (a) Abusleme, J.; Pieri, R.; Barchesi, E. (Sovay Solexis). International Patent WO 129041, 2008.(b) Galia, A.; Cipollina, A.; Scialdone, O.; Filardo, G. *J. Polym. Sci., Part A: Polym. Chem.* **2009**, *47*, 1034–1040.
(20) Ameduri, B.; Boyer, C. (Tosoh F-Tech, Inc.). JP 2008/214420, 2008.(b) Boyer, C.; Ameduri, B. *J. Polym. Sci., Part A: Polym. Chem.* **2009**, *47*, 4710–4722.
(21) (a) Asandei, A. D.; Chen, Y. Abstracts of Papers, 230th ACS National Meeting, Washington, DC, Aug. 28−Sept. 1, 2005, POLY-569 (*Polym. Prepr. Amer. Chem. Soc. Polym. Div.*). (b) Asandei, A. D.; Chen, Y. Abstracts of Papers, 234th ACS National Meeting, Boston, MA, August 19−23, 2007, POLY-127 (*Polym. Prepr. Amer. Chem. Soc. Polym. Div.*). (c) Asandei, A. D.; Chen, Y. Abstracts of Papers, 235th ACS National Meeting, New Orleans, LA, April 6−10, 2008, *Polym. Mater. Sci. Eng.-223*.
(22) (a) Lannuzel, T.; Guiot, J; Ameduri, B.; Boutevin, B. (Solvay S.A.). US 2006/160972, 2006.(b) Guiot, J; Ameduri, B.; Boutevin, B.; Lannuzel, T. *J. Polym. Sci., Part A: Polym. Chem.* **2006**, *44*, 3896–3910.
(23) (a) Ameduri, B.; Armand, M.; Boucher, M.; Manseri, A. (Hydro-Québec). U.S. Patent US 2007/185293, 2007.(b) Sauguet, L.; Boyer, C.; Ameduri, B.; Boutevin, B. *Macromolecules* **2006**, *39*, 9087–9101.
(24) Boyer, C.; Ameduri, B.; Boutevin, B.; Dolbier, W. R.; Winter, R.; Gard, G. *Macromolecules* **2008**, *41*, 1254–1263.
(25) Daikin. Japanese Patent 2000/0,228,218, 2000.
(26) Greenley, R. Z. Q and e Values for Free Radical Copolymerization of Vinyl Monomers and Telogens. In *Polymer Handbook*, 4th ed.; Abe, A.; Bloch, D. R.; Immergut, E. H.; Eds.; Wiley Intersciences: New York, 1999; Vol. *2*, pp 309−378.
(27) Ito, H.; Giese, B.; Engelbrecht, R. *Macromolecules* **1984**, *17*, 2204.
(28) McElroy, K. T.; Purrington, S. T.; Bumgardner, C. L.; Burgess, J. P. *J. Fluorine Chem.* **1999**, *95*, 117.
(29) David, G.; Boyer, C.; Tonnar, J.; Ameduri, B.; Lacroix-Desmazes, P.; Boutevin, B. *Chem. Rev.* **2006**, *106*, 3936–3962.
(30) Ameduri, B. *Macromolecules* **2010**, *43*, 10163–10184.
(31) (a) Alexandre, M.; Dubois, P. *Mater. Sci. Eng. Rep.* **2000**, *28*, 1–21. (b) Kang, S.; Hong, S. I.; Choe, C. R.; Park, M.; Rim, S. *Polymer* **2001**, *42*, 879–887. (c) Alexandre, M., Dubois, P. Nanocomposites (Chapter 1). In *Macromolecular Engineering. Precise Synthesis, Materials Properties, Applications*; Matyjaszewski, K., Gnanou, Y., Leibler, L., Eds.; Wiley-VCH: Weinheim, Germany, 2007; Vol. *4*, pp 4−38. (d) Paul, D. R.; Robeson, L. M. *Polymer* **2008**, *49*, 3187–3204.
(32) Liu, H. J.; Hwang, J. J.; Chen-Yang, Y. W. *J. Polym. Sci., Part A: Polym. Chem.* **2002**, *40*, 3873.
(33) (a) Priya, L.; Jog, J. P. *J. Polym. Sci., Part B: Polym. Phys.* **2002**, *40*, 1682. (b) Priya, L.; Jog, J. P. *J. Polym. Sci., Part B: Polym. Phys.* **2003**, *41*, 31.
(34) Priya, L.; Jog, J. P. *J. Appl. Polym. Sci.* **2003**, *89*, 2036.
(35) Dillon, D. R.; Tenneti, K. K.; Li, C. Y.; Ko, F. K.; Sics, I.; Hsiao, B. S. *Polymer* **2006**, *47*, 1678–1683.
(36) Zhang, Z.-C.; Wang, Z.; Chung, T. C. *Macromolecules* **2007**, *40*, 5235.
(37) Wu, C.-G.; Lua, M.-I.; Tsai, C.-C.; Chuang, H.-J. *J. Power Sources* **2006**, *159*, 295–300.
(38) Li, Z.; Su, G.; Wang, X.; Gao, D. *Solid State Ionics* **2005**, *176*, 1903–1908.
(39) Sel, O; Soules, A; Ameduri, B.; Boutevin, B.; Laberty Robert, C; Gebel, G.; Sanchez, C. *Adv. Funct. Mater.* **2010**, *20*, 1090–1098.
(40) Shah, D.; Maiti, P.; Gunn, E.; Schmidt, D. F.; Jiang, D. D.; Batt, C. A.; Giannelis, E. P. *Adv. Funct. Mat.* **2004**, *16*, 1173–1177.
(41) Shah, D.; Maiti, P.; Jiang, D. D.; Batt, C. A.; Giannelis, E. P. *Adv. Mater.* **2005**, *17*, 525–528.

(42) Yu, S.; Zuo, X.; Bao, R.; Xu, X.; Wang, J.; Xu, J. *Polymer* **2009**, *50*, 553–559.
(43) Huang, W.; Edenzon, K.; Fernandez, L.; Shabnam, R.; Woodburn, J.; Cebe, P. *J. Appl. Polym. Sci.* **2010**, *115*, 3238–3248.
(44) Ma, W.; Wang, X.; Zhang, J. *J. Polym. Sci., Part B: Polym. Phys.* **2010**, *48*, 2154–2164.
(45) Gohy, J.-F.; Levevre, N.; Hoeppener, S.; Schubert, U. S.; Kostov, G.; Ameduri, B. *Polym. Chem*., in press (doi: 10.1039/c0py00217h).
(46) Sawada, H. *Prog. Polym. Sci.* **2007**, *32*, 509–533. (b) Sawada, H. *Polym. J.* **2007**, *39*, 637–650.
(47) Sawada, H.; Kurachi, J.; Takahashi, H..; Ueno, K.; Hamazaki, K. *Polym. Adv. Technol.* **2005**, *16*, 651–654.
(48) Sawada, H.; Narumi, T.; Kajiwara, A.; Ueno, K.; Hamazaki, K. *Colloid Polym. Sci.* **2006**, *284*, 551–555.
(49) (a) Ito, H.; Okazaki, M.; Miller, D. C. *J. Polym. Sci., Part A: Polym. Chem.* **2004**, *42*, 1478–1505. (b) Ito, H.; Okazaki, M.; Miller, D. C. *J. Polym. Sci., Part A: Polym. Chem.* **2004**, *42*, 1506–1527. (c) Ito, H.; Trinque, B. C.; Kasai, P.; Willson, C. G. *J. Polym. Sci., Part A: Polym. Chem.* **2007**, *46*, 1559–1565.
(50) Mladenov, G.; Ameduri, B.; Kostov, G.; Mateva, R. *J. Polym. Sci., Part A: Polym. Chem.* **2006**, *44*, 1470–1485.
(51) (a) Hung, M.; Boyer, C.; Ameduri, B. (Dupont Performance Elastomer). U.S. Patent Application 2009/0105435 A1, 2009. (b) Boyer, C.; Ameduri, B.; Hung, M. *Macromolecules* **2010**, *43*, 3652–3660 .
(52) (a) Balague, J.; Ameduri, B.; Boutevin, B.; Caporiccio, G. *J. Fluorine Chem.* **1995**, *74*, 49–58. (b) Manseri, A.; Boulahia, D.; Ameduri, B.; Boutevin, B.; Caporiccio, G. *J. Fluorine Chem.* **1999**, *94*, 175–182.
(53) Boyer, C.; Valade, D.; Sauguet, L.; Ameduri, B.; Boutevin, B. *Macromolecules* **2005**, *38*, 10353–10362.
(54) Boyer, C.; Valade, D.; Lacroix-Desmazes, P.; Ameduri, B.; Boutevin, B. *J. Polym. Sci., Part A: Polym. Chem.* **2006**, *44*, 5763–5777.
(55) Tillet, G.; Boutevin, B.; Ameduri, B. *Prog. Polym. Sci.* **2011**, *36*, 191−217.
(56) Zeng, Q.; Stebbins, J. F. *Am. Mineral.* **2000**, *85*, 863 .
(57) Kao, H.-M.; Chen, Y.-C. *J. Phys. Chem. B* **2003**, *107*, 3367.
(58) Balague, J.; Ameduri, B.; Boutevin, B.; Caporiccio, G. *J. Fluorine Chem.* **2000**, *102*, 253–268.
(59) Sawada, H.; Narumi, T.; Kodama, S.; Kamijo, M.; Ebara, R.; Sugiya, M.; Iwasaki, Y. *Colloid Polym. Sci.* **2007**, *285*, 977–983.
(60) Sawada, H.; Tashima, T.; Kakehi, H.; Nishiyama, Y.; Kikuchi, M.; Miura, M.; Sato, Y.; Isu, N. *Polym. J.* **2010**, *42*, 167–171.
(61) Capron, P.; Ameduri B.; Boutevin, B.; Souzy, R. (Commissariat Energie Atomique). Eur. Patent EP 2008/0103003, 2008.